Electronic Supplementary Information (ESI) for Dalton Transactions

Two unprecedented decanuclear heterometallic $[Mn^{II}_2Mn^{III}_6Ln^{III}_2]$ (Ln = Dy, Tb) complexes displaying relaxation of magnetization †

Hui-Sheng Wang,[*a] Feng-Jun Yang,[a] Qiao-Qiao Long,[a] Zhi-Yong Huang,[a] Wei Chen,[a] Zhi-Quan Pan[a] and You Song[*b]

[a] School of Chemistry and Environmental Engineering, Wuhan Institute of Technology, Key Laboratory for Green Chemical Process of Ministry of Education, Wuhan 430074, P. R. China. Fax: +86-27-87194560

[b] State Key Laboratory of Coordinate Chemistry, Nanjing National Laboratory of Microstructures, School of Chemistry and Chemical Engineering, Nanjing University, Nanjing 210023, P. R. China.

Email: wangch198201@163.com (H.-S.Wang), yousong@nju.edu.cn (Y. S.)

Table S1 Crystallographic Data for **1** and **2**

Compounds	**1**	**2**
Formula[a]	$C_{92}H_{126}Dy_2Mn_8N_{18}O_{38}$	$C_{92}H_{126}Tb_2Mn_8N_{18}O_{38}$
Formula weight[a]	2856.62	2849.46
Crystal colour	Dark red	Dark red
Crystal size/mm	0.26 × 0.21 × 0.11	0.35 × 0.28 × 0.12
Crystal system	Monoclinic	Monoclinic
a(Å)	22.2955(10)	22.2950(11)
b(Å)	14.4552(6)	14.4491(8)
c (Å)	35.1699(16)	35.1815(18)
α(deg)	90.00	90.00
β(deg)	94.4780(10)	94.4410(1)
γ(deg)	90.00	90.00
Unit cell volume/Å^3	11300.2(9)	11299.4(10)
Temperature/K	173(2)	173(2)
Space group	C2/c	C2/c
Z	4	4
Radiation type	Mo/Kα	Mo/Kα
μ/mm^{-1}	2.254	2.184
D_c/g cm^{-3}	1.679	1.675
θ range	3.0702-24.8303	3.0686-25.3807
Index ranges	$-26 \le h \le 21$ $-17 \le k \le 14$ $-41 \le l \le 38$	$-26 \le h \le 20$ $-17 \le k \le 17$ $-35 \le l \le 41$
F(000)	5760	5752
Reflections collected	32988	43935
Unique reflections [R_{int}]	9857 [0.0549]	9786 [0.0494]
Reflections with $I > 2\sigma(I)$	6888	7454
Final R indices ($I > 2\sigma(I)$)[b,c]	$R_1 = 0.0427$ w$R_2 = 0.0764$	$R_1 = 0.0427$ w$R_2 = 0.0837$
Final R indices (all data)	$R_1 = 0.0820$ w$R_2 = 0.0839$	$R_1 = 0.0684$ w$R_2 = 0.0905$
S (all data)	1.023	1.022
$(\Delta\rho)_{max,min}$/e Å^{-3}	1.042 and -0.716	2.031 and -1.171

[a] The formula and the formula weights include the MeCN and H_2O solvent molecules which were free. [b] $R_1 = \Sigma(||F_o| - |F_c||)/\Sigma|F_o|$. [c] w$R_2 = [\Sigma[w(F_o^2 - F_c^2)^2]/\Sigma[w(F_o^2)^2]]^{1/2}$, $w = 1/[\sigma^2(F_o^2) + [(ap)^2 + bp]$, where $p = [\max(F_o^2, 0) + 2F_c^2]/3$.

Table S2 Selected bond lengths (Å) and angles (°) for **1**.

Bond lengths			
Dy(1)-O(19)	2.275(3)	Mn(2)-O(10)	2.188(3)
Dy(1)-O(15)	2.353(3)	Mn(2)-O(2)	2.241(3)
Dy(1)-O(17)	2.379(3)	Mn(2)-N(2)	2.261(4)
Dy(1)-O(14)	2.434(3)	Mn(2)-N(3)	2.369(4)
Dy(1)-O(13)	2.471(3)	Mn(3)-O(19)	1.825(3)
Dy(1)-O(18)	2.472(3)	Mn(3)-O(10)	1.901(3)
Dy(1)-O(16)	2.507(3)	Mn(3)-O(2)	1.948(3)
Dy(1)-N(6)	2.635(4)	Mn(3)-O(13)	1.977(3)
Dy(1)-N(5)	2.660(4)	Mn(3)-O(9)	2.143(3)
Mn(1)-O(7)	1.886(3)	Mn(3)-O(1)	2.394(3)
Mn(1)-O(1)	1.911(3)	Mn(4)-O(19)	1.834(3)
Mn(1)-O(17)	1.943(3)	Mn(4)-O(11)	1.921(3)
Mn(1)-N(1)	2.055(4)	Mn(4)-O(15)[a]	1.937(3)
Mn(1)-O(5)	2.159(4)	Mn(4)-O(18)	1.960(3)
Mn(1)-O(13)	2.333(3)	Mn(4)-O(18)[a]	2.309(3)
Mn(2)-O(8)	2.125(3)	Mn(4)-N(4)	2.414(4)
Mn(2)-O(3)	2.145(4)		
Bond angles			
O(19)-Dy(1)-O(17)	83.32(10)	O(3)-Mn(2)-O(10)	153.18(13)
O(15)-Dy(1)-O(17)	165.51(11)	O(3)-Mn(2)-O(2)	134.08(13)
O(19)-Dy(1)-O(14)	147.15(11)	O(10)-Mn(2)-O(2)	70.22(11)
O(15)-Dy(1)-O(14)	120.43(10)	O(10)-Mn(2)-N(2)	89.75(13)
O(17)-Dy(1)-O(18)	102.67(10)	O(19)-Mn(3)-O(10)	95.93(13)
N(6)-Dy(1)-N(5)	137.58(12)	O(19)-Mn(3)-O(2)	172.79(13)
O(16)-Dy(1)-N(6)	62.52(11)	O(10)-Mn(3)-O(2)	82.89(13)
O(19)-Dy(1)-N(5)	108.95(11)	O(19)-Mn(3)-O(1)	110.58(12)
O(7)-Mn(1)-O(1)	170.42(14)	O(13)-Mn(3)-O(1)	77.60(12)
O(7)-Mn(1)-O(17)	92.67(13)	O(9)-Mn(3)-O(1)	148.58(12)
O(1)-Mn(1)-N(1)	81.25(15)	O(19)-Mn(4)-O(11)	94.97(13)
O(17)-Mn(1)-O(5)	98.75(13)	O(19)-Mn(4)-O(15)[a]	174.06(14)
N(1)-Mn(1)-O(5)	90.20(15)	O(11)-Mn(4) -O(15)[a]	90.54(12)
O(17)-Mn(1)-O(13)	78.13(12)	O(19)-Mn(4)-O(18)	81.95(13)
O(8)-Mn(2)-O(3)	97.71(14)	O(19)-Mn(4)-N(4)	90.25(13)
O(8)-Mn(2)-O(10)	92.81(12)	O(11)-Mn(4)-N(4)	74.42(13)

Symmetry code: a 0.5-x, 1.5-y, -z

Table S3 Selected bond lengths (Å) and angles (°) for **2**.

Bond lengths			
Mn(1)-O(17)	1.836(3)	Mn(3)-O(4)	2.403(3)
Mn(1)-O(1)	1.924(3)	Mn(4)-O(18)	1.883(3)
Mn(1)-O(15)[a]	1.945(3)	Mn(4)-O(4)	1.917(3)
Mn(1)-O(11)	1.973(3)	Mn(4)-O(13)	1.941(3)
Mn(1)-O(11)[a]	2.317(3)	Mn(4)-N(4)	2.057(4)
Mn(1)-N(1)	2.410(4)	Mn(4)-O(9)	2.163(4)
Mn(2)-O(7)	2.129(3)	Mn(4)-O(16)	2.334(3)
Mn(2)-O(5)	2.156(4)	Tb(1)-O(11)	2.478(3)
Mn(2)-O(2)	2.192(3)	Tb(1)- O(12)	2.516(3)
Mn(2)-O(3)	2.248(3)	Tb(1)- O(13)	2.391(3)
Mn(2)-N(3)	2.265(4)	Tb(1)- O(14)	2.459(3)
Mn(2)-N(2)	2.363(4)	Tb(1)-O(15)	2.362(3)
Mn(3)-O(17)	1.822(3)	Tb(1)- O(16)	2.474(3)
Mn(3)-O(2)	1.904(3)	Tb(1)- O(17)	2.286(3)
Mn(3)-O(3)	1.943(3)	Tb(1)- N(5)	2.644(4)
Mn(3)-O(16)	1.985(3)	Tb(1)- N(6)	2.665(4)
Mn(3)-O(8)	2.143(3)		
Bond angles			
O(17)-Mn(1)-O(1)	94.85(13)	O(3)-Mn(3)-O(4)	62.56(12)
O(17)-Mn(1)-O(15)[a]	173.97(14)	O(8)-Mn(3)-O(4)	148.62(12)
O(1)-Mn(1)-O(15)[a]	90.61(13)	O(18)-Mn(4)-O(4)	170.57(15)
O(17)-Mn(1)-O(11)	82.18(13)	O(18)-Mn(4)-O(13)	92.76(14)
O(17)-Mn(1)-N(1)	90.45(14)	O(4)-Mn(4)-N(4)	81.45(15)
O(1)-Mn(1)-N(1)	74.41(13)	O(13)-Mn(4)-O(9)	98.85(14)
O(5)-Mn(2)-O(2)	152.95(15)	O(4)-Mn(4)-O(16)	80.37(12)
O(7)-Mn(2)-O(3)	89.82(13)	O(13)-Mn(4)-O(16)	78.25(12)
O(5)-Mn(2)-O(3)	134.39(14)	O(17)-Tb(1)-O(13)	83.45(11)
O(2)-Mn(2)-O(3)	70.02(11)	O(15)-Tb(1)-O(13)	165.49(11)
O(7)-Mn(2)-N(2)	98.68(14)	O(17)-Tb(1)-O(14)	147.13(11)
N(3)-Mn(2)-N(2)	99.92(14)	O(15)-Tb(1)-O(14)	120.53(11)
O(17)-Mn(3)-O(2)	95.87(13)	O(13)-Tb(1)-O(14)	73.33(11)
O(17)-Mn(3)-O(3)	172.64(14)	O(17)-Tb(1)-O(16)	64.70(10)
O(2)-Mn(3)-O(3)	82.95(13)	O(17)-Tb(1)-N(5)	113.49(11)
O(17) -Mn(3)-O(4)	110.48(13)	O(13)-Tb(1)-N(6)	119.20(11)

Symmetry code: a 0.5-x, 1.5-y, -z

Table S4 Calculating bond valences by using the bond valence sum (BVS) method

Atom	+2	+3	+4
Mn1	3.15	2.91	3.00
Mn2	1.90	1.77	1.81
Mn3	3.26	2.98	3.13
Mn4	3.15	2.89	3.02

Table S5 The possible geometries of nonacoordination metal centers.

geometry	point group	polyhedron
EP-9	D_{9h}	Enneagon
OPY-9	C_{8v}	Octagonal pyramid
HBPY-9	D_{7h}	Heptagonal bipyramid
JTC-9	C_{3v}	Johnson triangular cupola J3
JCCU-9	C_{4v}	Capped cube J8
CCU-9	C_{4v}	Spherical-relaxed capped cube
JCSAPR-9	C_{4v}	Capped square antiprism J10
CSAPR-9	C_{4v}	Spherical capped square antiprism
JTCTPR-9	D_{3h}	Tricapped trigonal prism J51
TCTPR-9	D_{3h}	Spherical tricapped trigonal prism
JTDIC-9	C_{3v}	Tridiminished icosahedron J63
HH-9	C_{2v}	Hula-hoop
MFF-9	C_s	Muffin

Table S6 Deviation parameters calculated by *SHAPE* from each ideal polyhedron for complexes **1** and **2**.

Structure	**1**	**2**
EP-9	45.998	46.246
OPY-9	36.695	35.624
HBPY-9	30.214	30.527
JTC-9	26.989	25.856
JCCU-9	25.391	24.935
CCU-9	26.290	25.745
JCSAPR-9	23.054	22.659
CSAPR-9	23.541	23.490
JTCTPR-9	23.471	23.481
TCTPR-9	24.256	24.175
JTDIC-9	29.560	29.145
HH-9	26.997	26.625
MFF-9	22.893	22.732

Table S7 The value of A and B by performing linear approximation for different frequency.

frequency (Hz)	$\tau_0 \times 10^9$ (s)	E_a (K)
111	1.034	20.94
511	1.080	20.84
711	2.734	18.344
1111	2.315	18.50
2111	1.969	18.55
3111	2.318	17.72
4111	1.401	18.93
5111	1.039	19.45
7111	2.659	16.28
9111	0.5445	20.21

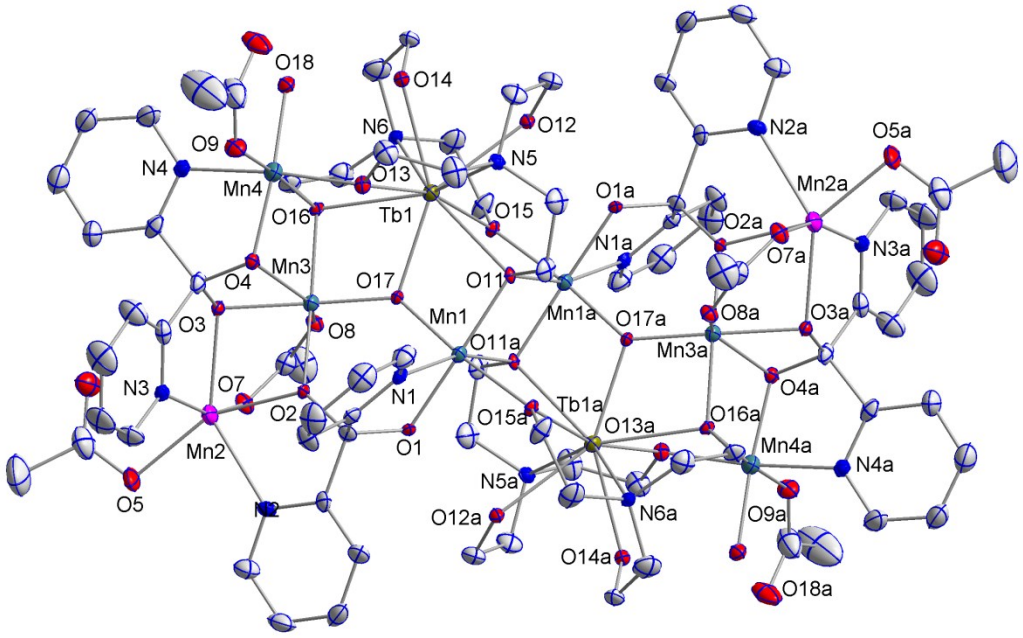

Fig. S1 ORTEP representation of compound **2** with the thermal ellipsoids of non-metal and metal atoms at 30% and 50% probability, respectively. For clarity, the H atoms and the noncoordinated solvent molecules are omitted (symmetry code: a 0.5-x, 1.5-y, -z), Mn^{II} pink, Mn^{III} teal, Tb^{III} dark yellow, O red, N blue, C gray.

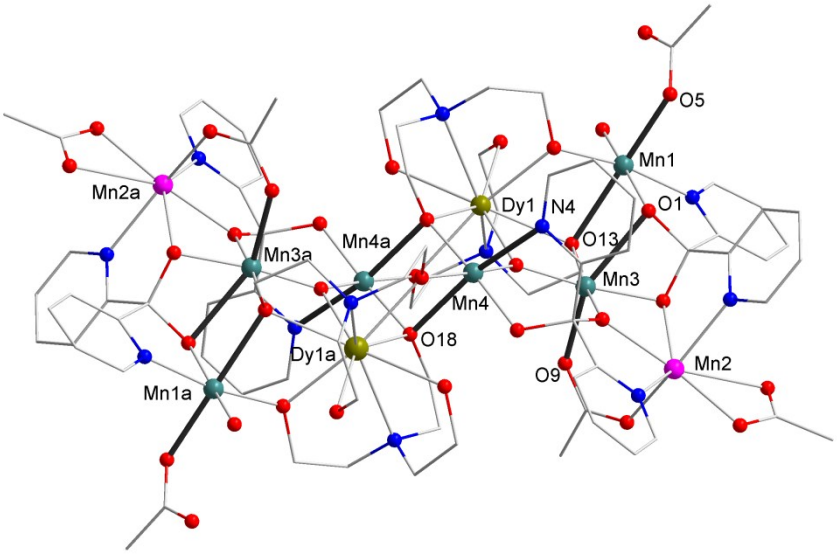

Fig. S2 Black lines showing the Jahn-Teller axes of Mn^{III} in complex **1,** symmetry code: a 0.5-x, 1.5-y, -z.

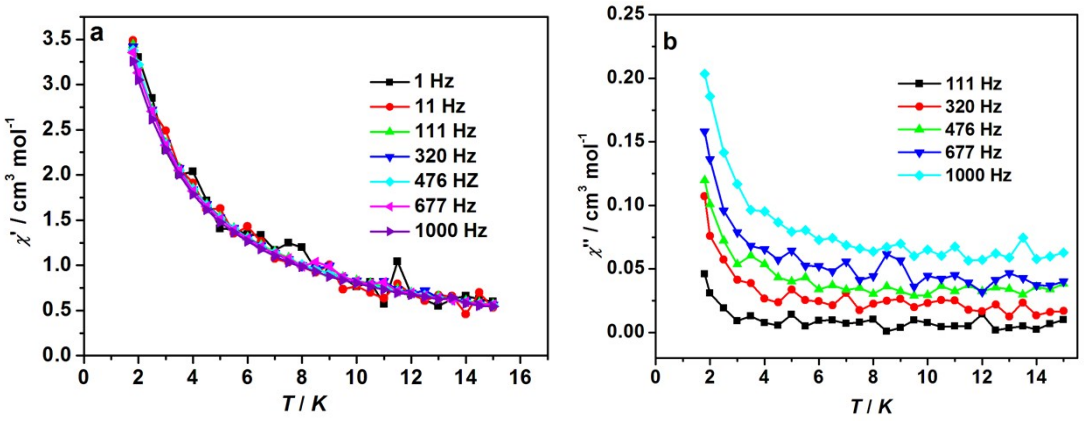

Fig. S3. Temperature dependence of the in-phase χ_M' (a) and out-of-phase χ_M'' (b) in a 5 Oe ac field oscillating at 1-1000 Hz with a zero applied dc field for **1**.

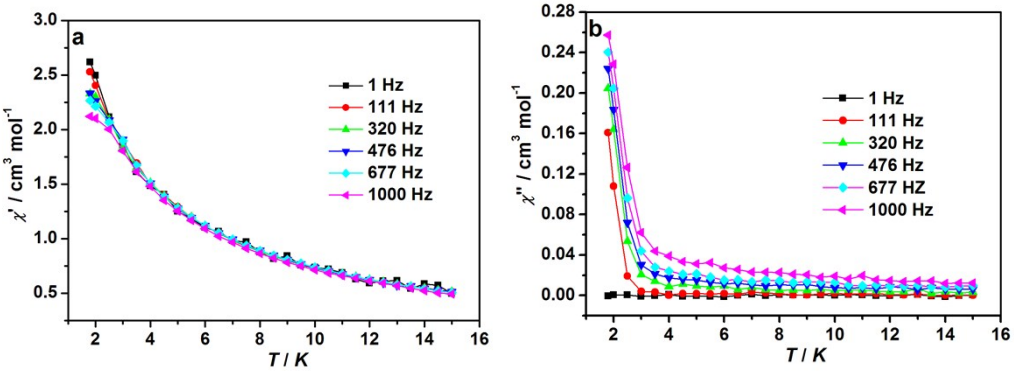

Fig. S4 Temperature dependence of the in-phase χ_M' (a) and out-of-phase χ_M'' (b) in a 5 Oe ac field oscillating at 1-1000 Hz with a zero applied dc field for **2**.

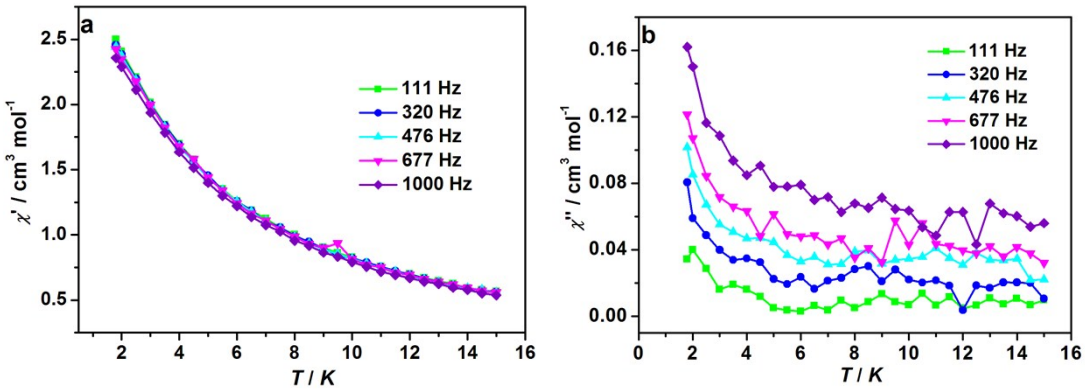

Fig. S5. Temperature dependence of the in-phase χ_M' (a) and out-of-phase χ_M'' (b) in a 5 Oe ac field oscillating at 111-1000 Hz with a 2000 Oe applied dc field for **1**.

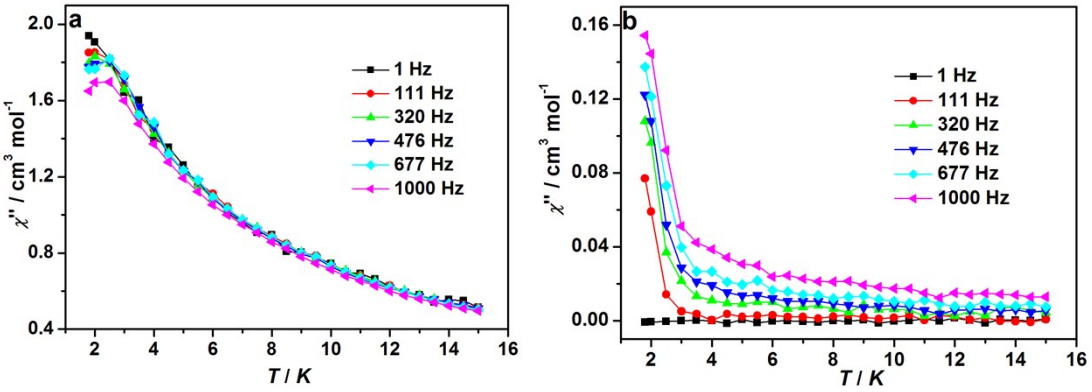

Fig. S6. Temperature dependence of the in-phase χ_M' (a) and out-of-phase χ_M'' (b) in a 5 Oe ac field oscillating at 111-1000 Hz with a 2000 Oe applied dc field for **2**.